

Chapter 4 Seepage Problems

Seepage problems involve the analysis of the flow of groundwater through porous media such as soil and rock. Geotechnical engineers typically perform seepage analyses as part of the design process for embankment dams, levees, and river structures such as locks and dams.

4-1. Results and Uses of Seepage Analyses

The principal quantity solved for in a finite element solution of a seepage problem is the pressure head at each nodal point in the finite element mesh. All flow is assumed to occur through the pore spaces of a rigid soil skeleton. From these heads, the quantity and velocity of flow, and hydraulic gradients at any point in the system can be determined. Flow nets can be constructed from the finite element results to help the design engineer interpret the results.

4-2. Types of Seepage Analyses

a. Seepage problems. Seepage problems can be classified according to the type of flow conditions presumed to exist for the analysis. The analyses of most seepage problems for engineering projects are performed under the assumption of *steady-state* flow conditions. This assumption implies that all conditions affecting the flow of water through the system are the same at all times, hence the solution is independent of time. In contrast, *transient* solutions to seepage problems, performed less frequently, are time-dependent as factors such as changing headwater and tailwater levels and the flow of water into partially saturated soils can be accounted for in this type of analysis.

b. Confined or unconfined seepage problems. Seepage problems can also be classified as confined or unconfined depending on the boundary conditions presumed to exist. In confined flow problems, the locations of all boundaries are known and fixed. Unconfined flow problems must have at least one impervious boundary and a free surface boundary. The location of the free surface boundary (phreatic surface) is unknown and must be determined as part of the solution. Boundary conditions are presumed to be impervious to flow.

4-3. Constitutive Law and Material Properties

a. Darcy's law. The constitutive relationship in most finite element codes is based on Darcy's law. Darcy's law states that the velocity of the fluid is proportional to the hydraulic gradient. The constant of proportionality in this relationship is termed the coefficient of permeability. This coefficient is a parameter which is material dependent. Most finite element codes are capable of handling materials having anisotropic permeabilities.

The coefficient of permeability is typically estimated in three different ways:

(1) Sampling and laboratory testing. Sampling and laboratory testing where samples retrieved from a field exploration program are sent to the laboratory where permeability tests can be performed. The two most common types of laboratory permeability tests are the constant head and falling head types of tests.

(2) Correlations with grain-size distribution. For example, the Lower Mississippi Valley Division of the Corps of Engineers has correlated the grain-size distribution of sands in the Lower Mississippi Valley to the coefficient of permeability. This relationship is shown in Figure 33.

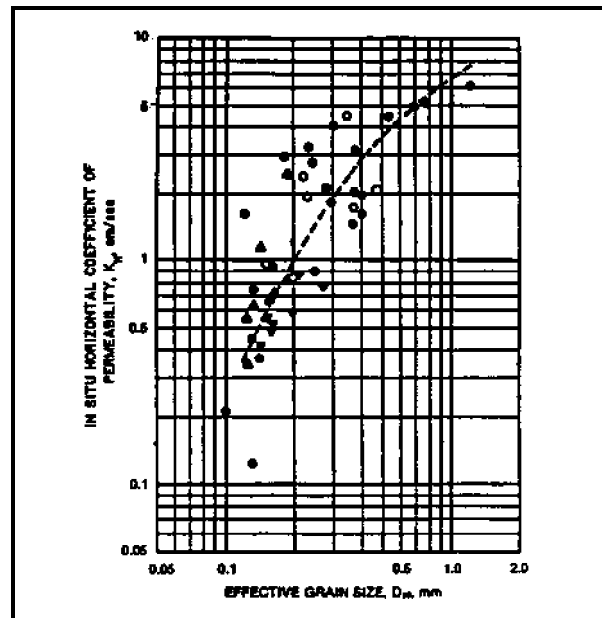


Figure 33. Relationship between in situ horizontal permeability and effective size

(3) Field tests. Permeability can be estimated from field pump tests and falling head tests performed in boreholes.

b. *Documented reference.* Engineer Manual EM 1110-2-1901 entitled "Seepage Analysis and Control for Dams" contains more detailed information on the methods for determining the coefficient of permeability.

4-4. Case History: S. A. Murray Hydroelectric Plant

a. *Project description.* A 2-D plan view seepage analysis of the S. A. Murray, Jr. Hydroelectric Station was reported by Knowles (1992). The power plant is adjacent to the Mississippi River just upstream from the Old River Control Structure.

Plan and cross-sectional views of the site are shown in Figures 34 and 35. The powerplant is founded in a medium to very dense layer of fine to medium

sand, approximately 100 ft deep. Below this sand layer is hard tertiary clay. A channel was cut from the Mississippi River through the mainline levee to divert flow to the powerplant. An exit channel leads flow away to auxiliary overflow channels. The entire site is surrounded by a levee system which ties into the mainline levee and the natural levee and backswamp deposits.

b. *Purpose of analysis.* As shown in Figure 34, the powerplant receives flow from the Mississippi River through a diversion channel and could experience differential hydraulic heads up to 26 ft from project flood conditions and 41 ft under extreme conditions. These heads cause seepage to occur under the structure and subject it to uplift pressures. Seepage control measures include concrete cutoff walls and a drainage system. These cutoff walls under the structure extend through the sand layer to the tertiary deposits. The analysis was performed to determine the seepage and associated uplift pressure beneath the powerplant and other structural features (e.g. concrete channel linings) and to study the effect of the cutoff walls on the seepage.

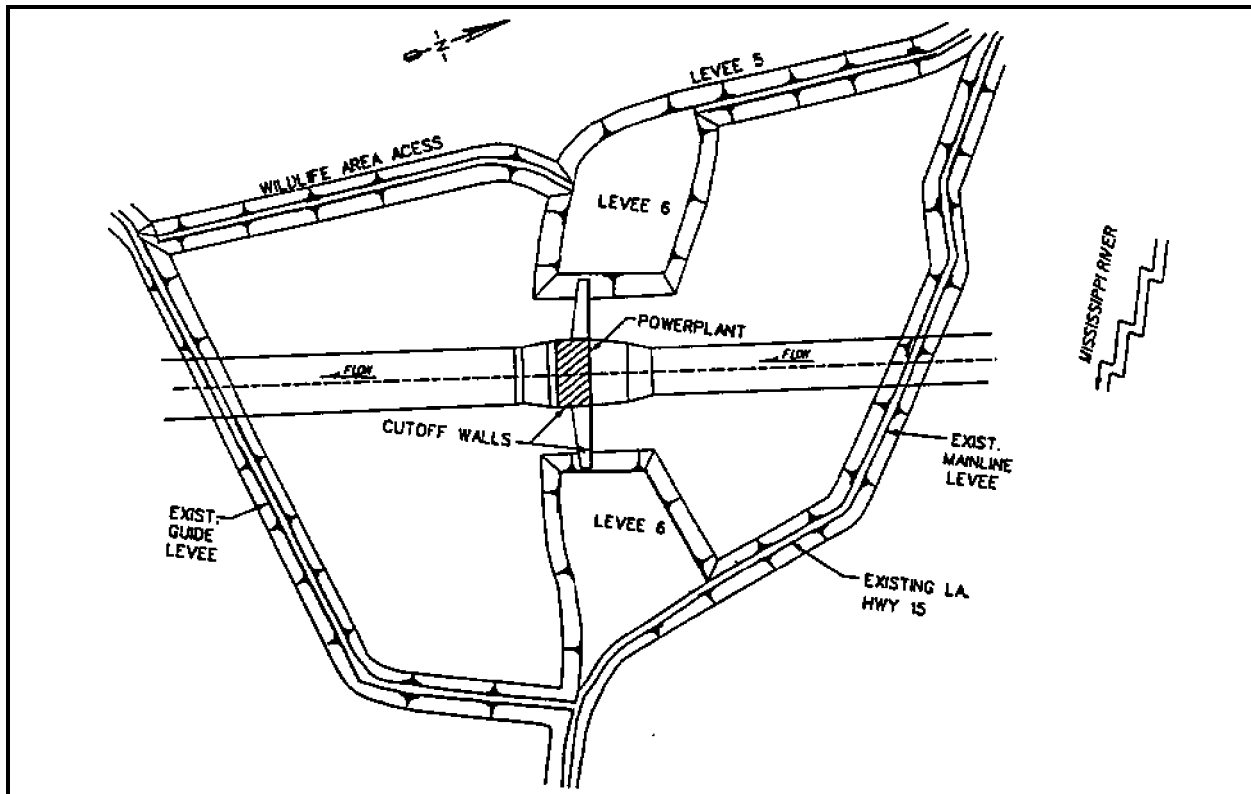


Figure 34. Plan view of S. A. Murray Hydroelectric Plant

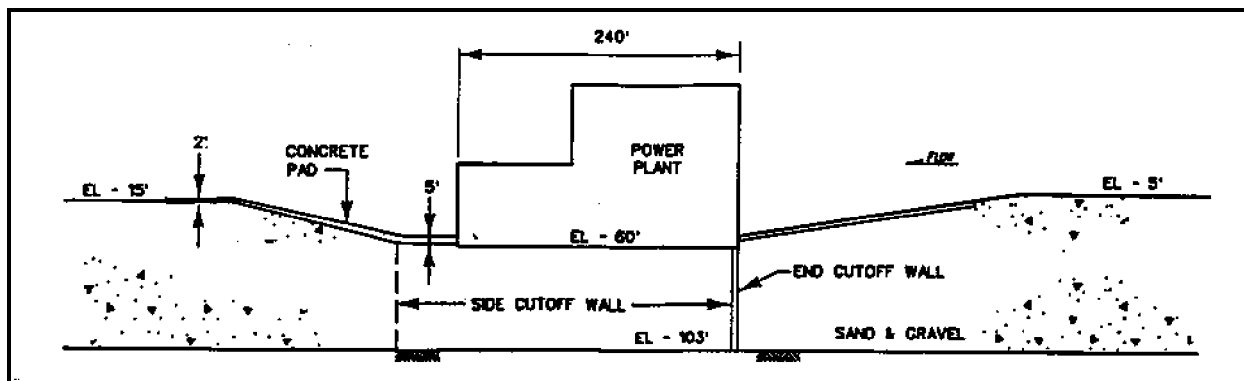


Figure 35. Section view through centerline of powerplant

c. *Finite element model, code, and material properties.* The program CSEEP (Tracy 1983) was to assess the uplift pressure on the structure from a plan view model. Two simplifying assumptions were made so that the problem could be solved as a 2-D problem. First, it was assumed to be a confined flow problem. The ground surface adjacent to the structure and channels is covered by a natural clay and silt blanket or by a man-made clay blanket. These make the surface of the surrounding area highly impermeable, therefore, water will flow mainly from the upstream channel and the surrounding subsurface stratum under the structure to the downstream channel. The second assumption is that the seepage occurs in one uniformly thick layer having a constant permeability. Figure 36 shows the finite element mesh used in the analysis. The boundaries were chosen so they would not unduly influence the seepage pattern around the power plant. The boundary conditions (shown in Figure 36) were selected to represent a piezometric level equal to the water level of the Mississippi River. The extreme differential hydraulic head conditions, 41 ft, were applied in these analyses. The soil is considered to be homogeneous and isotropic with a permeability of 0.14 ft/min. The design permeability for the cutoff wall was 2×10^{-6} ft/min. The effect of the cutoff walls on the seepage was of particular interest with respect to the resulting uplift pressures under the powerplant and downstream lining. Several analyses were performed in which the permeability of the cutoff walls was varied from 10^{-6} to 10^{-2} ft/min to determine the range of effectiveness of the cutoff walls in controlling uplift pressures.

d. *Results.* Figure 37 shows a vector plot of flow for the case of the cutoff walls having a permeability of 2×10^{-6} ft/min. Most flow occurs around the cutoff walls from upstream to downstream with

little under the structure itself. Contours of total head for this case are shown in Figure 38. Most head drop occurs along the walls outside of the powerplant structure and downstream channel lining. The uplift pressure distribution along the centerline of the structure is plotted in Figure 39 for this case. Uplift pressures resulting from the various cutoff wall permeabilities used in the parametric study are shown in Figure 40. At the highest permeability of 10^{-2} ft/min, the distribution of head is nearly linear under the structure. Another analysis performed in which the cutoff wall was modeled as impervious (zero permeability) gave results which were almost identical to the results for 10^{-6} ft/min. The results of the analysis clearly display the influence of the cutoff wall on the uplift under the structure. The design permeability makes the cutoff wall act as a relatively impervious barrier causing water to flow around the structure resulting in a longer flow path and reduced uplift pressures under the structure. Conversely, with the highest permeability, 10^{-2} ft/min, the wall hardly impedes flow at all because this value is near the same order of permeability as the surrounding soil, 10^{-1} ft/min.

4-5. Case History: Cerrillos Dam

a. *Project description.* Palmerton (1993) reported on a 3-D steady-state seepage analysis of Cerrillos Dam near Ponce, Puerto Rico, for the U.S. Army Engineer District, Jacksonville. Cerrillos Dam is 323 ft high and has a crest length of 1,555 ft. The dam consists of a central clay core, a grout curtain extending to a depth of 200 ft, and upstream and downstream rockfill shells with the appropriate transition zones. The geologic structure near the dam is characterized by steeply dipping planar and parallel

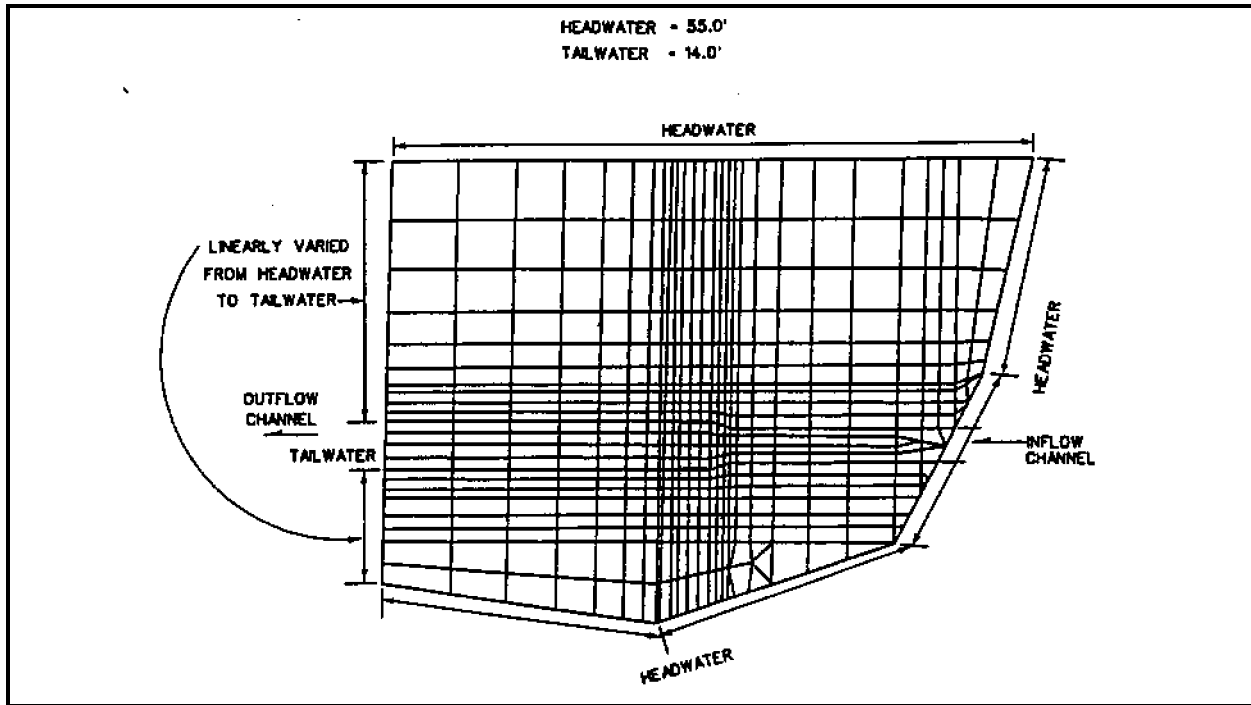


Figure 36. Grid generated for plan view model of S. A. Murray Hydroelectric Plant

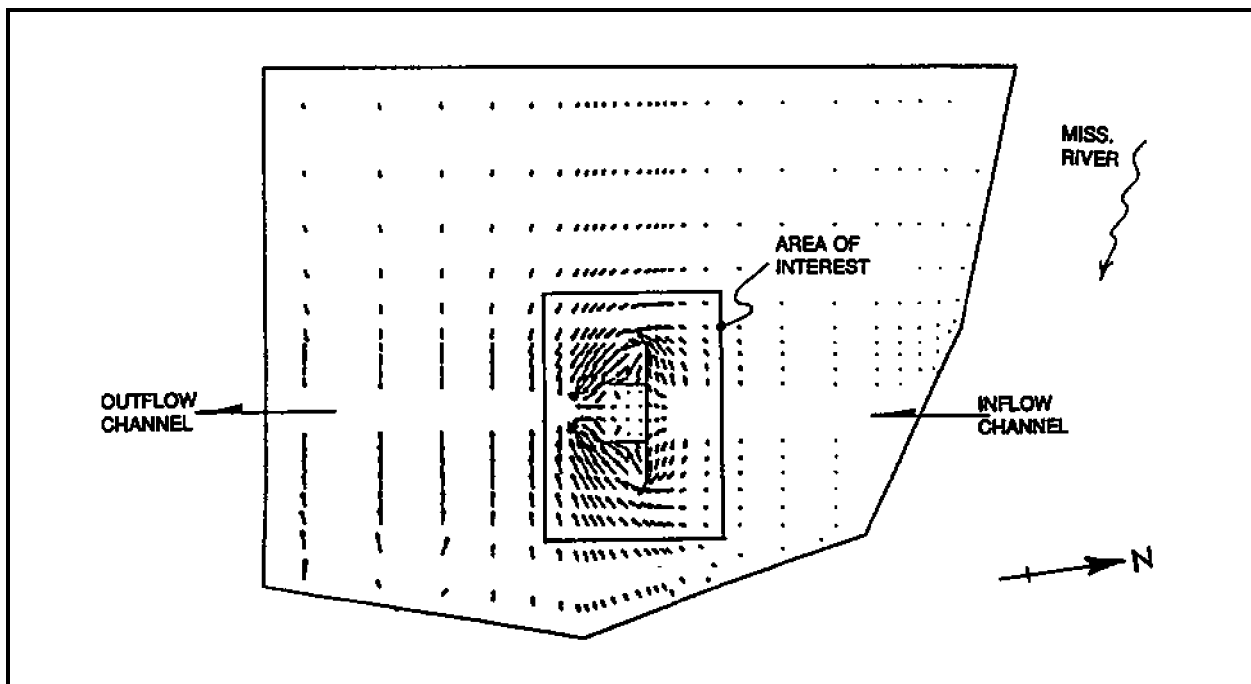


Figure 37. Flow velocity vectors with the cutoff wall at a permeability of 2×10^{-6} ft/min

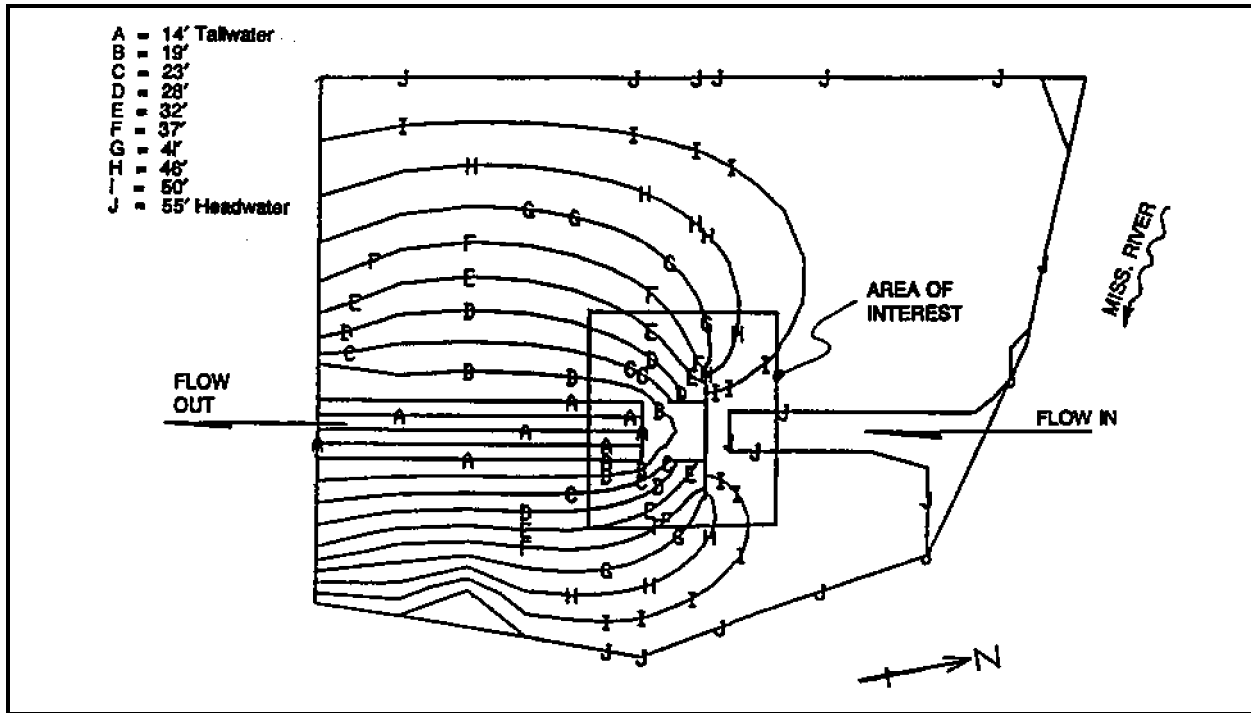


Figure 38. Total head contours with cutoff wall at a permeability of 2×10^{-6} ft/min

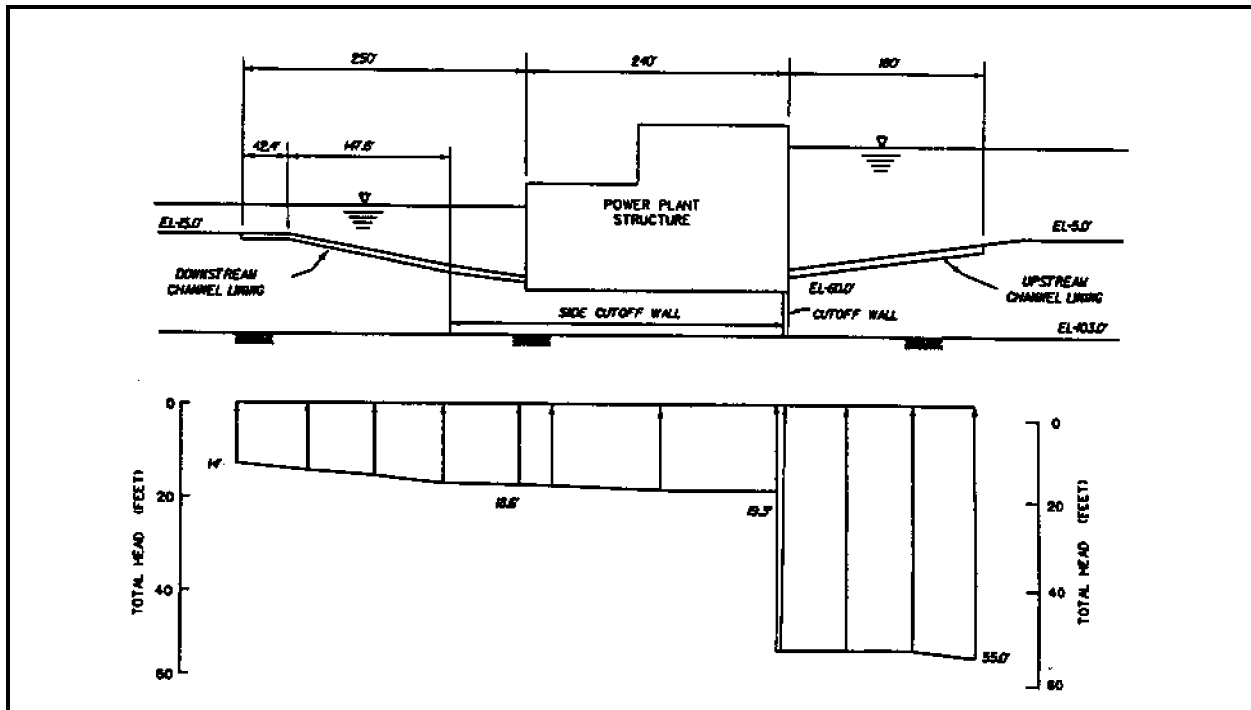


Figure 39. Uplift at centerline of powerplant with cutoff wall permeability of 2×10^{-6} ft/min

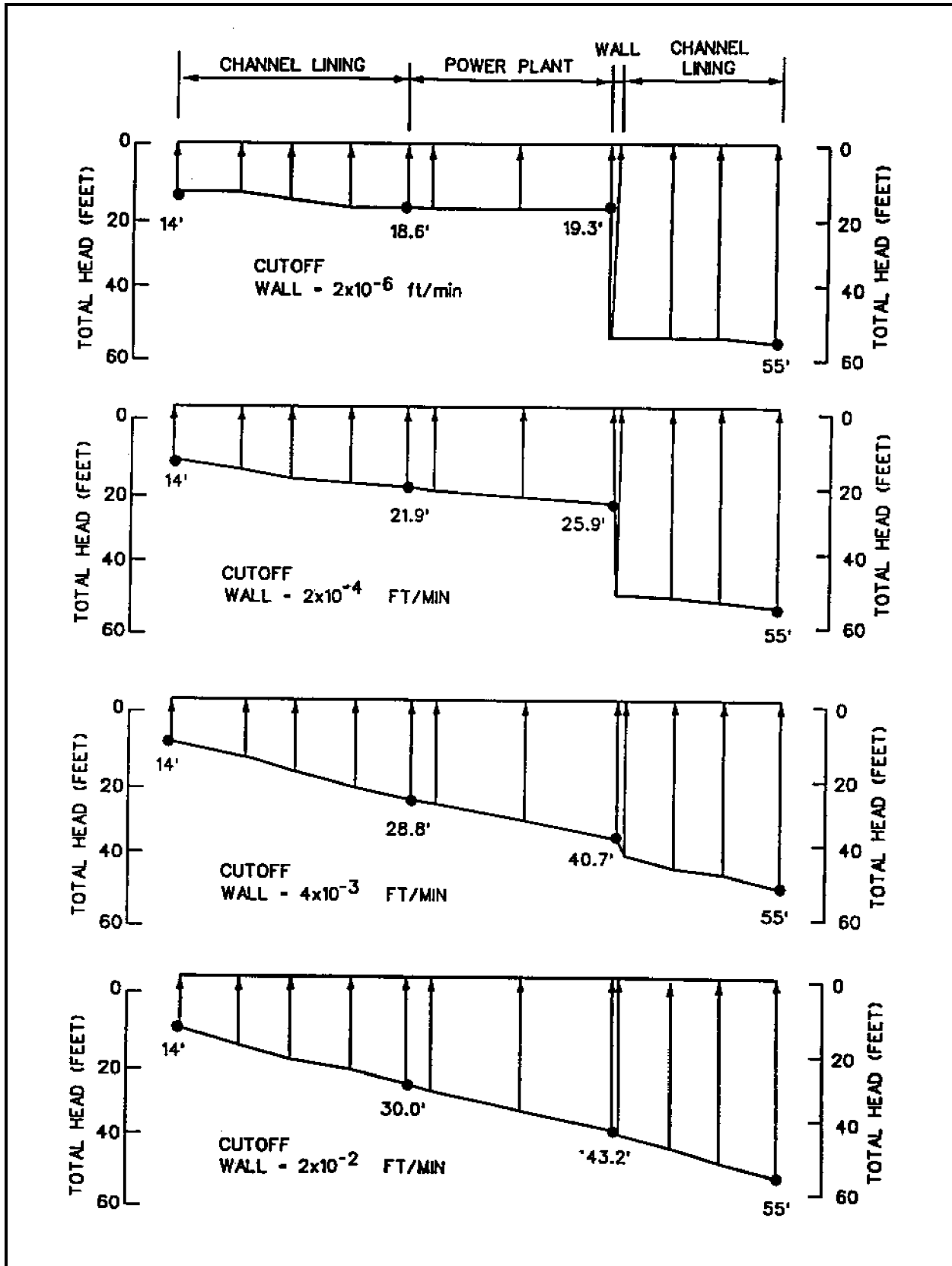


Figure 40. Uplift at centerline of powerplant and channel linings for a range of cutoff wall permeabilities

units of limestone, siltstones, and tuff. Of these, the Ridge Limestone Unit is the most pervious. The Ridge Limestone Unit outcrops on the left valley wall at the dam's abutment. The 3-D spatial relationships between the Ridge Limestone Unit and the components of the embankment dam are shown in Figures 41 and 42. These figures show that at the left abutment different portions of the Ridge Limestone Unit are exposed or are in contact with the upstream rockfill shell, the impervious core, and the grout curtain. Water from the reservoir was believed to enter the Ridge Limestone Unit on the left abutment where it moved beneath the grout curtain and into the seepage collection system located on the downstream side of the dam.

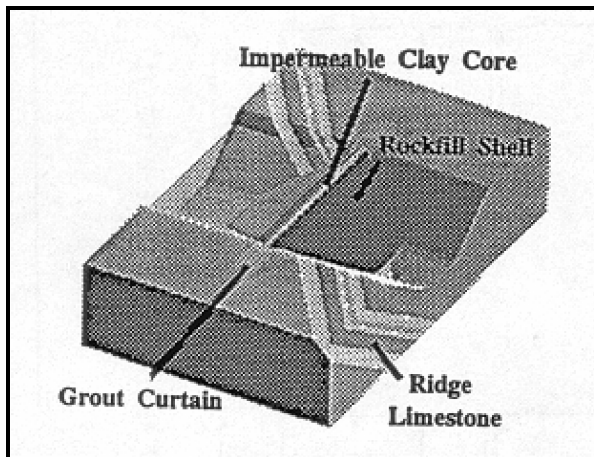


Figure 41. Simplified 3-D model dam, grout curtain, and Ridge Limestone

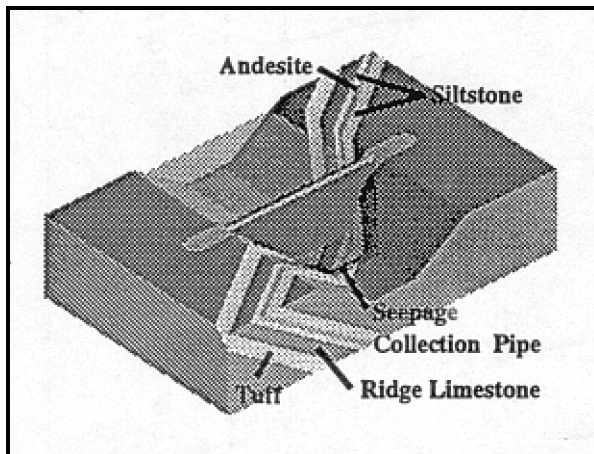


Figure 42. View showing geology at Cerrillos Dam (rockfill shells are transparent)

b. *Purpose.* The 3-D finite element analyses was performed because the quantity of seepage, 4 cfs, after the first reservoir filling when the pool was at el 495 (depth of 200 ft) exceeded the design estimate of 1 cfs. The initial estimate was based on a 2-D hand drawn flow net analysis which was not able to account for the complex geological conditions at the site. The 3-D analysis was performed to overcome this limitation and gain an improved understanding of the flow conditions. After validating the 3-D model against the observed flow quantities the model was used to predict seepage quantities at different pool elevations and evaluate the effectiveness of potential remedial measures.

c. *Finite element model.* Palmerton used the 3-D finite element code, CSEEP3D, developed by Tracy (1991) to perform his analysis. The problem was treated as a steady-state unconfined flow problem. The methods developed for pre- and post-processing for this problem were critical to the success of this study due to the large size of the finite element simulation. A grid generator program was written specifically for this study to develop the mesh shown in Figure 43 as the task of manually constructing the 3-D mesh for a problem of this size would be overwhelming. Different finite element meshes were used depending upon the pool elevation made for a particular run. For example, for the case where the pool is 350 ft deep, the generated mesh contained 8,282 elements and 10,810 nodal points. All meshes for this study were based on the idealized section shown in Figure 44. The output file from the finite

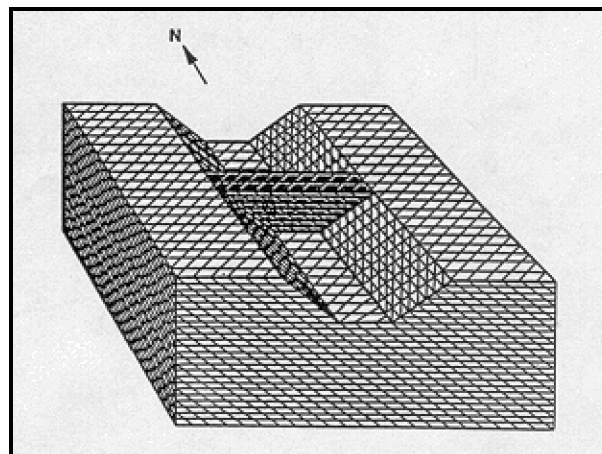


Figure 43. 3-D finite element mesh

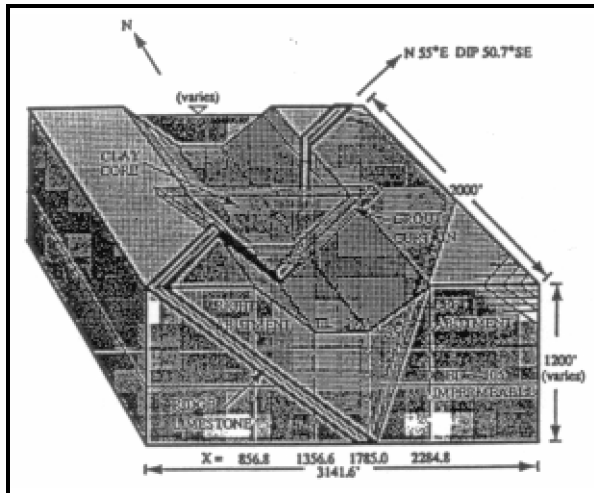


Figure 44. Pertinent dimensions and features of 3-D finite element mesh

element runs were very extensive. Computer routines were developed to extract piezometric heads, flows, and the position of the phreatic surface from the output of the 3-D seepage code. The permeabilities used in this analysis are listed in Table 1.

Table 1. Permeabilities of Materials for Cerrillos Dam

Material	Permeability (cm/sec)
Grout Curtain	1.0×10^{-6} cm/sec
Impermeable clay core of dam	6.4×10^{-7} cm/sec
Ridge Limestone Unit	5.0×10^{-3} cm/sec
All other foundation rock units above el -105 ft	1.0×10^{-4} cm/sec
All foundation rock units below el -105 ft	Impermeable

Palmerton concluded that 3-D finite element solutions offer an effective engineering approach toward the evaluation of proposed corrective measures for reducing or controlling seepage under and through embankment dams where conditions warrant accounting for

3-D effects. Additionally, he recommended the use of 2-D finite element analysis for 2-D situations because of the limitations and oversimplifications

inherent in the conventional flow net analysis which is performed manually. Palmerton noted that for "situations where multiple zones and anisotropic permeability must be included, a numerical model is, for all practical purposes, mandated."

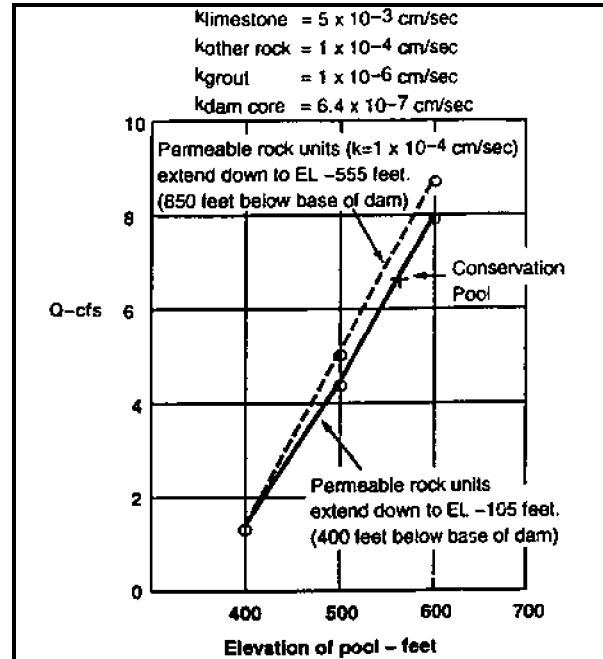


Figure 45. Predicted seepage discharges for various pool levels from 3-D FE analysis

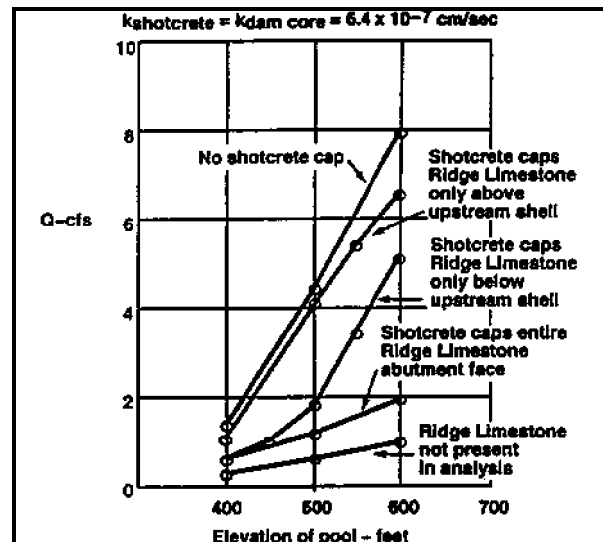


Figure 46. Effect of shotcrete placement on left valley wall

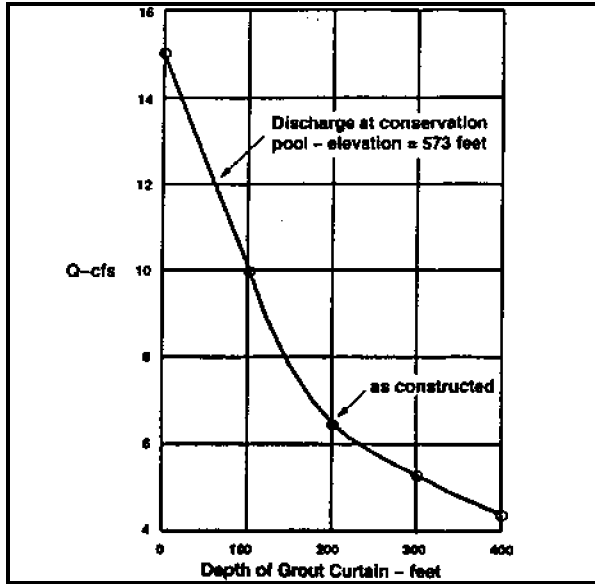


Figure 47. Effect of deepening grout curtain